To follow the fate of fibroblasts after their incorporation into the lattice, we labeled them with [^{3}H]thymidine. A segment of each graft was taken at the time of implantation so that estimates of cell density and of the proportion of labeled cells could be made at the outset. Labeled cells were still seen in grafts recovered after 7 days (Fig. 2), but the total number of cells in the graft had increased greatly as a result of cell division or cell migration into the graft or both. The number of labeled cells in 10-day-old grafts was similiar to that in 6- or 7-day-old grafts, but after 5 weeks very few labeled cells were detected.

There are two possible explanations for their decreased presence. The first is that many of the original cells died or emigrated and were replaced by cells that migrated into the graft from the surrounding tissue; the second is that the cells of the graft underwent numerous divisions, diluting the isotope to the point where disintegrations were too few to be detected after a 3-week exposure.

The organization of the graft in the rat superficially resembles that of normal surrounding tissue, except that hair follicles and sebaceous glands are absent. Fibroblasts are distributed throughout, with intercellular matrix separating the cells. The matrix of the graft can be distinguished from that of adjacent tissue when sections are examined with polarization optics. While the matrix of normal tissue is highly birefringent, birefringence is substantially reduced in the graft but does increase with graft age. As early as 1 week the graft shows areas of birefringence, a phenomenon not observed so early in granulation tissue. Initially, collagen fibrils appear to lie mainly parallel to the skin surface along a single axis of orientation. The typical woven appearance of the collagen mat is barely apparent after 7 weeks. Even after 9 weeks it is still not well developed. We do not know whether longer-term grafts will exhibit a normal dermis or whether its development depends on the technique of lattice casting.

After 10 weeks the average thickness of the graft dermis measured about half that of the adjacent dermis, which was about 1.3 mm. The dermis of the graft appeared much less spongy and more compact than that of adjacent skin; however, in the zone of transition between them, the dermis was spongier. Also, the graft dermis was more birefringent in the transition zone than anywhere else.

In most of the grafts we examined, the panniculus layer normally found underlying the dermis was absent; loose connective tissue with many adipose cells was present instead. We assume that the panniculus had retracted when the graft site was prepared. Vascularization of the grafts was evident after 7 days (Fig. 2b). After 5 weeks the grafts were well vascularized, and no ischemic regions were apparent. By 7 weeks the vascular development of the graft was similiar to that of the surrounding tissue.

The skin-equivalent graft, unlike epidermis alone (*4*, *5*), acts as a skin graft of full thickness. And the graft, whether partly or entirely remodeled, persists, since after many months it can be distinguished as a hairless area comparable in size to the original wound. Although there is doubt about the source of the dermal cells that populate the grafts after several months, it is clear that the implanted tissue is vascularized, inhibits wound contraction, fills the original wound, and eventually resembles skin in many respects.

Our approach provides for the fabrication of skin-equivalent tissue in virtually unlimited amounts from a small biopsy, since it depends mainly on replication in vitro of the required number of dermal and epidermal cells. Although we have successfully used rat collagen as a lattice for grafts composed of guinea pig cells, we have not yet tested the acceptability of grafts in which collagen from more remote species is used.

We think that the most crucial prerequisite for graft acceptance is contraction and conditioning of the lattice by cells from the individual who will receive the graft. The practical uses of the skin-equivalent graft are obvious, particularly since the substance can be cast into virtually any shape. However, its potential for reducing distortion and functional impairment in human injuries requiring skin replacement remains to be established.

EUGENE BELL
Department of Biology, Massachusetts Institute of Technology, Cambridge 02139
H. PAUL EHRLICH
Department of Pathology, Harvard Medical School, Massachusetts General Hospital, Shriners Burns Institute, Boston 02114
DAVID J. BUTTLE
Shriners Burns Institute
TAKAKO NAKATSUJI
Department of Biology, Massachusetts Institute of Technology

References and Notes

1. E. Bell, B. Ivarsson, C. Merrill, *Proc. Natl. Acad. Sci. U.S.A.* **76**, 1274 (1979).
2. E. Bell, C. Merrill, D. Solomon, *J. Cell Biol.* **83**, 398 (Abstr.) (1979).
3. S. Sher, B. Hull, R. Sarber, E. Bell, in preparation.
4. R. E. Billingham and P. B. Medawar, *J. Anat.* **89**, 114 (1955).
5. R. E. Billingham and P. S. Russell, *Ann. Surg.* **144**, 961 (1956).
6. W. L. McKeehan, *Cell Biol. Int. Rep.* **1**, 335 (1977).
7. We thank R. Trelstad for advice and consultations on graft histology. This study was supported in part by grants from Flow Laboratories to E.B. and by PHS grant GN25561 to H.P.E.

5 November 1980

Separation of Calcium Isotopes by Liquid Phase Thermal Diffusion

Abstract. *Significant separation of the isotopes of calcium was obtained by thermogravitational thermal diffusion of an aqueous calcium nitrate solution. A flow of solvent was used to partially offset the large solute-solvent separation effect in the experimental column. Further development of this technique may lead to separation of the isotopes of calcium and of other elements on a practical scale.*

Thermogravitational thermal diffusion in the liquid phase (*1*) was first applied to the large-scale separation of uranium isotopes by Abelson *et al.* (*2*). It has been used recently to separate practical quantities of sulfur (*3*), chlorine (*4*), and bromine (*5*) isotopes. Many elements, however, do not have stable, low-molecular-weight, liquid compounds in a temperature range suitable for thermal diffusion separation. In principle, it is possible to separate these elemental systems as solutions of some solid compound in a suitable solvent. Normally, the separation of solute from solvent is much greater than the separation of isotopic species; therefore, in an efficient thermal diffusion column nearly pure solvent accumulates at one end of the system and essentially all of the solute concentrates at the other end.

For nonisotopic systems, Korsching (*6*) demonstrated that the solvent-solute separation could be suppressed by imposing a net flow of solvent through the separation column. It can be shown (*7*) that in a dilute solution the solvent flow does not affect the separation of the components of the solute. In this report we describe the separation of calcium isotopes by the Korsching technique and derive some conditions necessary for its successful application.

If we consider the system at first as a

0036-8075/81/0306-1054$00.50/0

two-component system, solvent and solute, we can write the following equation for net transport of solvent through the system (*8*):

$$\tau_1 = H_{ss} w_1(1 - w_1) - K \frac{dw_1}{dz} + \sigma w_1 \quad (1)$$

where τ_1 is the net transport, H_{ss} the initial transport coefficient for the solute-solvent pair, w_1 the mass fraction of solvent, K the remixing coefficient, z the vertical coordinate, and σ the net mass flow through the column. Noting that σ equals the solvent injection rate and that $\tau_1 = \sigma$ at the steady state, we have

$$\frac{dw_1}{dz} = \frac{(H_{ss} w_1 - \sigma)(1 - w_1)}{K} \quad (2)$$

Thus the solvent concentration gradient can be eliminated by choosing the solvent injection rate such that

$$\sigma = H_{ss} w_1 \quad (3)$$

It is well known that the thermal diffusion column is extremely susceptible to superimposed parasitic circulations, which tend to destroy the separation effect. We would expect instability and large-scale parasitic circulation to occur if

$$\frac{d\rho}{dz} > 0 \quad (4)$$

where ρ is the fluid density. For systems such as aqueous salt solutions this would result when

$$\frac{dw_1}{dz} < 0 \quad (5)$$

or when

$$\sigma > H_{ss} w_1 \quad (6)$$

Calcium nitrate was chosen for our experiments on the basis of its high solubility in water and compatibility with materials of construction (austenitic stainless steel). The thermal diffusion column had the following dimensions: length, 72 cm; hot- to cold-wall spacing, 254 μm; and average circumference, 8 cm. The column was heated by steam at 164°C and the cooling water temperature was 30°C. The estimated effective temperature difference across the working fluid was 100°C.

A preliminary experiment without solvent injection was performed to permit estimation of the column coefficients for the solute-solvent separation. The experiment, which was done in the transient mode, indicated that H_{ss} was strongly dependent on concentration, with a range from about 4×10^{-4} g/sec at a $Ca(NO_3)_2$ concentration of 30 percent by weight to 2×10^{-3} g/sec at infinite dilution. The equilibrium separation factor for the solute-solvent pair was approximately 5000.

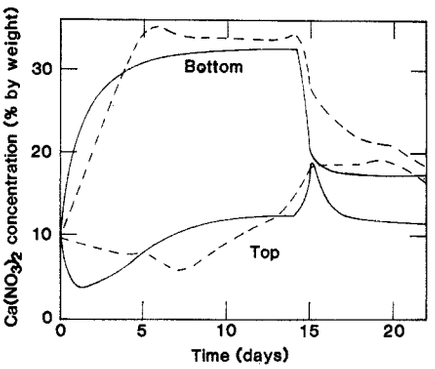

Fig. 1. Solute concentration during the calcium isotope separation experiment. Dashed lines are experimental data; solid lines are calculated from the solution of Eq. 7.

Experiments with solvent flow were set up with the same column. The concept was that of Korsching, but solvent evaporation was replaced by continuous feed of a concentrated solution of material of natural isotopic abundance to the top of the column accompanied by continuous withdrawal of relatively more dilute material at the same location. If allowed to proceed indefinitely, this would lead to (i) an isotopic composition at the top of the column approaching natural abundance and (ii) a solute concentration at the top consistent with a material balance for the several flows.

The column was filled with a 10 percent (by weight) aqueous solution of $Ca(NO_3)_2$. Separation was allowed to proceed for several hours without external flow in order to establish a stable density gradient. Then the several flows were established at the following rates: solvent (water) feed to the bottom of the column, 0.24 g/hour; 40 percent solution feed to the top of the column, 0.11 g/hour; and top outflow, 0.35 g/hour. We attempted to hold these conditions steady for the next 14 days; however, some variation was unavoidable, and it may have amounted to as much as ±20 percent in the feed rate of concentrated solution.

Solute concentrations during the experiment are shown in Fig. 1 along with values calculated from a finite-difference solution of the time-dependent transport equation (*8*)

$$\frac{\partial w_1}{\partial t} = -\frac{1}{\mu} \frac{\partial \tau_1}{\partial z} \quad (7)$$

where t is time and μ is column holdup per unit length. To model the observed behavior theoretically, it was necessary to use values of H_{ss} somewhat smaller than the estimates derived from the transient experiment. This is not particularly surprising in view of the crude nature of the procedure used to generate the data. The solvent injection rate was below that required to completely offset the solute concentration gradient; however, it was sufficient to sustain a useful solute concentration at the top of the column.

Samples were taken for calcium isotope ratio determinations on days 12, 13, and 14. Results are given in Table 1. The isotopic separation is, as expected, mass-dependent, with the separation of the ^{40}Ca-^{48}Ca pair showing the largest effect. The effect is similar in magnitude to isotope effects obtained without solvent injection in aqueous solutions of other

Table 1. Separation of calcium isotopes in an aqueous solution of $Ca(NO_3)_2$. Samples were taken from the top or the bottom of the column as indicated.

Time (days)	Position	Isotopic composition (atom percent)			
		^{42}Ca	^{43}Ca	^{44}Ca	^{48}Ca
Feed		0.62	0.125	1.88	0.152
		Solvent flow: 0.24 g/hour			
12	Top	0.60	0.117	1.78	0.136
	Bottom	0.64	0.134	2.00	0.168
13	Top	0.60	0.120	1.77	0.135
	Bottom	0.64	0.136	2.01	0.170
14	Top	0.60	0.123	1.77	0.137
	Bottom	0.64	0.133	2.02	0.173
		Solvent flow: 0.60 g/hour			
18	Top	0.62	0.128	1.88	0.151
	Bottom	0.64	0.133	2.01	0.175
19	Top	0.63	0.129	1.89	0.152
	Bottom	0.64	0.132	2.00	0.172
20	Top	0.61	0.127	1.87	0.153
	Bottom	0.64	0.132	2.02	0.175
21	Top	0.62	0.128	1.87	0.150
	Bottom	0.64	0.134	2.02	0.174
23	Top	0.62	0.128	1.87	0.150
	Bottom	0.64	0.132	2.04	0.177

elements (*2, 7, 9-11*). It seems to be large enough to support separation of calcium isotopes on a practical scale by the solvent flow technique.

An attempt to reduce the solute concentration gradient by increasing solvent flow was only partly successful. On day 14 the flow rates were increased to the following values: solvent feed, 0.60 g/hour; 40 percent solution feed, 0.25 g/hour; and top outflow, 0.85 g/hour. As indicated in Fig. 1, the solute concentration gradient did decrease, but the results were somewhat out of line with those predicted. A detailed examination of the composition profiles calculated from theory showed that a clearly defined positive concentration gradient would develop during the transition period following the change in conditions. This would be expected to lead to at least partial remixing of the column contents. As expected under these conditions, the isotope separation dropped somewhat. The results are equivalent to an average separation factor of 1.16 for the ^{40}Ca-^{48}Ca pair, as opposed to the value of 1.26 obtained during the first 14 days of the experiment.

Further development of this technique may lead to a practical process for separating isotopes in solution and thus to improved availability of calcium and other isotopes to the scientific community. It is already established that the thermal diffusion method is well suited to moderate-scale enrichment of noble gas isotopes and to enrichment of the isotopes of elements, such as sulfur and chlorine, that form simple stable liquid compounds over an appropriate temperature range.

W. M. RUTHERFORD
K. W. LAUGHLIN

Mound Facility,
Monsanto Research Corporation,
Miamisburg, Ohio 45342

References and Notes

1. K. F. Alexander, *Fortschr. Phys.* **8**, 1 (1960).
2. P. H. Abelson, N. Rosen, J. I. Hoover, "Liquid thermal diffusion," *U.S.A.E.C. Rep. TID-5229* (1958).
3. W. M. Rutherford, *Ind. Eng. Chem. Process Des. Dev.* **17**, 77 (1978).
4. _____, *U.S. Dept. Energy Rep. MLM-2654* (1979).
5. G. D. Rabinovich, R. Ya Gurevich, V. P. Ivaknik, *Teplo Massoperenos Dokl. Vses. Soveshch. 4th* **4**, 401 (1972).
6. H. Korsching, *Z. Naturforsch. Teil B* **7**, 187 (1951).
7. G. D. Rabinovich, V. I. Shinkevich, K. K. Azroyan, *Inzh. Fiz. Zh.* **37**, 76 (1979).
8. W. M. Rutherford, *Sep. Purif. Methods* **4**, 305 (1975).
9. H. Korsching and K. Wirtz, *Naturwissenschaften* **27**, 367 (1939).
10. G. Panson, thesis, Columbia University (1953).
11. P. Varga-Manyi, *Acta Biochim. Biophys. Acad. Sci. Hung.* **1**, 197 (1966).
12. Mound Facility is operated for the Department of Energy under contract DE-AC04-76DP00053. We acknowledge the contributions of S. J. Evans to the early phase of this work.

22 September 1980; revised 5 December 1980

Phase Shifting Circadian Rhythms Produces Retrograde Amnesia

Abstract. *Phase shifting circadian rhythms in rats shortly after passive avoidance training impaired their performance on retention tests. The amnesia was not due to simple performance deficits accompanying the "jet lag" effects of phase shifting or to differences in lighting or circadian phase at training and at testing. Amnesia was associated with specific rhythm reentrainment patterns. These data indicate that disrupting circadian organization can produce retrograde amnesia in rats.*

Circadian organization may be an important factor in memory processes. Performance on retention tests in a variety of appetitive and aversive tasks fluctuates rhythmically, with optimal retention occurring 24 hours after training (*1, 2*). These fluctuations in retention appear to depend on the integrity of circadian rhythms (*3*). Many processes that influence memory (brain protein synthesis, neural activity, synaptic excitability, neurotransmitter synthesis, and hormone secretion) display circadian oscillations (*4*). It is likely that the rhythms governing such processes account for periodic fluctuations in retention and for the circadian variations in the effectiveness of treatments, such as electroconvulsive shock (*5*), that affect memory.

It is difficult to evaluate the importance of rhythmic organization for memory processing, since prior research has been purely correlational, implicating internal rhythms indirectly or inferentially. Retention fluctuations may reflect widespread rhythms in processes that influence memory. But rhythmic organization may be a prerequisite for normal memory. Assessment of the relative importance of circadian organization in normal memory requires that retention be examined after some direct manipulation of circadian rhythms. The most effective way to alter circadian rhythms is to change, or phase-shift, the light cycle that entrains them.

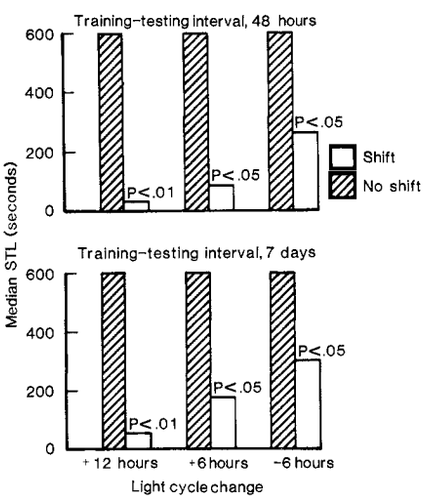

Fig. 1. Retention performance of rats in a one-trial passive avoidance task (maximum retention score, 600 seconds). No two groups, experimental or control, differed significantly in their training STL's, which were almost always less than 60 seconds. All animals were trained in light and placed in darkness immediately afterward. After training, light cycle changes were accomplished by varying the onset of the next light cycle. Positive phase shifts indicate phase advances; that is, the next light cycle began earlier than usual. The negative phase shift indicates a phase delay; the onset of the next light cycle began later than usual.

Male albino rats weighing between 200 and 400 g were housed individually in clear plastic cages, put on a 12-hour light-dark cycle (lights on from 0800 to 2000 hours), and given unrestricted access to food and water. Activity was recorded when a rat broke either of two photocell beams (*6*) that traversed its cage longitudinally. Activity counts were accumulated and recorded every 10 minutes. Circadian activity rhythms were used to monitor the progress of the phase shift (*7*).

The rats were trained between 0830 and 1030 hours in a one-trial passive avoidance task (*8*). The trough-shaped apparatus consisted of a brightly lit start box and a larger, unlit shock box. The rat was placed in the start box facing away from a circular door to the shock box. When it stepped into the far end of the shock box, a shock generator-scrambler (BRS SGS-001) delivered current (0.1 W for 5 seconds) through steel plates in the shock-box floor. After stepping into the shock box, receiving shock, and escaping back into the start box, the rat was returned to its home cage. Testing was identical to training except that no shock was delivered. Passive avoidance was indexed by the length of time each rat took to step into the shock box. This step-through latency (STL) and the shock-box escape latency were recorded automatically by electronic timers. If a rat did not enter the shock box within 600 seconds an arbitrary STL of 600 seconds was recorded. Low testing STL's were interpreted as poor retention. We examined eight phase shift conditions, each of which was paired with a control (no shift) condition ($N = 8$ rats per group).

Circadian rhythms were phase-shifted by turning off the home-cage lights immediately after training. The rats were

0036-8075/81/0306-1056$00.50/0